



Department of Energy

Washington, DC 20585

QA: N/A

DOCKET NUMBER: 63-001

January 29, 2010

ATTN: Document Control Desk

John H. (Jack) Sulima, Project Manager
Project Management Branch B
Division of High-Level Waste Repository Safety
Office of Nuclear Material Safety and Safeguards
U.S. Nuclear Regulatory Commission
EBB-2B2
11545 Rockville Pike
Rockville, MD 20852-2738



YUCCA MOUNTAIN - REQUEST FOR ADDITIONAL INFORMATION - SAFETY
EVALUATION REPORT, VOLUME 3 -POSTCLOSURE CHAPTER 2.2.1.3.2,
MECHANICAL DISRUPTION OF ENGINEERED BARRIERS, 4TH SET - (DEPARTMENT
OF ENERGY'S SAFETY ANALYSIS REPORT SECTION 2.3.4)

Reference: Ltr, Sulima to Williams, dtd 12/14/2009, "Yucca Mountain – Request for
Additional Information – Safety Evaluation Report, Volume 3 – Postclosure
Chapter 2.2.1.3.2, Mechanical Disruption of Engineered Barriers, 4th Set –
(Department of Energy's Safety Analysis Report Section 2.3.4)"

The purpose of this letter is to transmit the U.S. Department of Energy's (DOE) responses to two
(2) of the three (3) Requests for Additional Information (RAI) identified in the above-referenced
letter. The responses to RAI Numbers 1 and 2 are provided as an enclosure to this letter. DOE
expects to submit the remaining response on or before February 10, 2010.

The DOE references cited in the RAI response have previously been provided with the License
Application (LA) or the LA update.

There are no commitments in the enclosed RAI responses. If you have any questions regarding
this letter, please contact me at (202) 586-9620, or by email to jeff.williams@rw.doe.gov.


 Jeffrey R. Williams, Supervisor
Licensing Interactions Branch
Regulatory Affairs Division
Office of Technical Management

OTM:CJM-0256

Enclosures:

Response to RAI Volume 3, Chapter 2.2.1.3.2, Set 4, Number 1 and 2



cc w/encls:

J. C. Chen, NRC, Rockville, MD
J. R. Cuadrado, NRC, Rockville, MD
J. R. Davis, NRC, Rockville, MD
R. K. Johnson, NRC, Rockville, MD
A. S. Mohseni, NRC, Rockville, MD
N. K. Stablein, NRC, Rockville, MD
D. B. Spitzberg, NRC, Arlington, TX
J. D. Parrott, NRC, Las Vegas, NV
L. M. Willoughby, NRC, Las Vegas, NV
Jack Sulima, NRC, Rockville, MD
Christian Jacobs, NRC, Rockville, MD
Lola Gomez, NRC, Rockville, MD
W. C. Patrick, CNWRA, San Antonio, TX
Budhi Sagar, CNWRA, San Antonio, TX
Beverly Street, CNWRA, San Antonio, TX
Rod McCullum, NEI, Washington, DC
B. J. Garrick, NWTRB, Arlington, VA
Bruce Breslow, State of Nevada, Carson City, NV
Alan Kalt, Churchill County, Fallon, NV
Irene Navis, Clark County, Las Vegas, NV
Ed Mueller, Esmeralda County, Goldfield, NV
Ron Damele, Eureka County, Eureka, NV
Alisa Lembke, Inyo County, Independence, CA
Chuck Chapin, Lander County, Battle Mountain, NV
Connie Simkins, Lincoln County, Pioche, NV
Linda Mathias, Mineral County, Hawthorne, NV
Darrell Lacy, Nye County, Pahrump, NV
Jeff VanNeil, Nye County, Pahrump, NV
Joe Kennedy, Timbisha Shoshone Tribe, Death Valley, CA
Mike Simon, White Pine County, Ely, NV
K. W. Bell, California Energy Commission, Sacramento, CA
Barbara Byron, California Energy Commission, Sacramento, CA
Susan Durbin, California Attorney General's Office, Sacramento, CA
Charles Fitzpatrick, Egan, Fitzpatrick, Malsch, PLLC

EIE Document Components:

001_Trans_Ltr_3.2.2.1.3.2_Set_4_RAI_1_2.pdf	
002_Encl_3.2.2.1.3.2_Set_4_RAI_1_2_Part1of4.pdf	9,064 KB
003_Encl_3.2.2.1.3.2_Set_4_RAI_1_2_Part2of4.pdf	6,278 KB
004_Encl_3.2.2.1.3.2_Set_4_RAI_1_2_Part3of4.pdf	15,648 KB
005_Encl_3.2.2.1.3.2_Set_4_RAI_1_2_Part4of4.pdf	9,146 KB

RAI Volume 3, Chapter 2.2.1.3.2, Fourth Set, Number 1:

Explain how the cumulative effects of thermal stress and initial seismic events are considered in analyses of the extent of rockfall from multiple seismic events and affect repository performance.

Basis: In addition to forming a small amount of rockfall, DOE analyses show that a 10^{-4} seismic event creates block interfaces that have failed in shear or tension (e.g., BSC, 2004, Figure 6-120). Based on the DOE UDEC-Voronoi model calibration, such block failures should reduce the strength of the rock mass. However, an analysis of multiple 10^{-4} seismic events in a heated drift (BSC, 2004, Figure S-49) shows the same amount of rockfall as occurs in a single 10^{-4} seismic event in a heated drift (BSC, 2004, Figure S-47). DOE has not explained how the apparent weakening in rock strength from an initial seismic event, especially in the area close to the drift opening (e.g., BSC, 2004, Figure 6-120), stabilizes the rock mass such that no additional rockfall occurs during a subsequent seismic event. This result also does not appear consistent with caving relationships in BSC (2004, Figure 6-149), which show that caving potential increases as the hydraulic radius of the opening increases.

1. RESPONSE**1.1 APPROACH FOR ANALYSIS OF CUMULATIVE EFFECTS**

Different loading scenarios were considered in the analysis of drift degradation in the lithophysal rock mass, including: (1) combined effects of thermally induced stresses and seismic events¹ with relatively high probability of exceedance (BSC 2004, Section 6.4.2.3.2) and (2) combined effects of time-dependent strength degradation, thermally induced stresses, and multiple seismic events (BSC 2004, Section S3.4.3). Only the relatively high probability seismic events with 10^{-4} probability of annual exceedance were considered, combined with the thermally induced stresses and the time-dependent strength degradation. Because the effect of stronger events (i.e., 10^{-5} or lower probability of annual exceedance) on the drift stability is much greater than the effect of thermally induced stresses and the time-dependent strength degradation, those loading conditions were not considered combined. For example, the events with 10^{-6} or lower probability of annual exceedance cause complete drift collapse in the lithophysal rock mass, so thermal stress or

¹ The term “seismic event” in this response generally refers to the ground motion caused by an earthquake. In the context of postclosure seismic consequence analyses, the ground motion is typically characterized by the peak ground velocity (PGV) value of its first horizontal component. For a given value of horizontal PGV, the probabilistic seismic hazard analysis for Yucca Mountain, combined with ground motion conditioning and site-response modeling, gives a mean annual frequency with which the peak velocity value is expected to be exceeded (the bounded hazard curve). Seismic event rates refer, therefore, to ground motion exceedance rates rather than earthquake occurrence rates. For convenience, sets of three-component ground motion time histories are sometimes referred to in terms of their horizontal PGV value (e.g., 0.4 m/s PGV ground motions) or the mean annual frequency of the horizontal PGV value being exceeded (e.g., 10^{-4} ground motions).

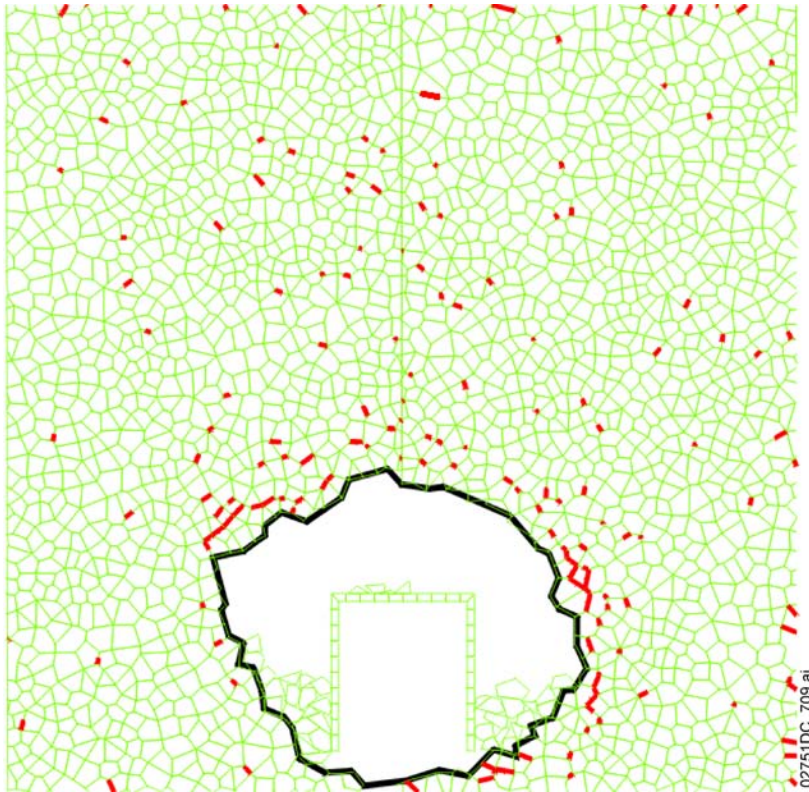
strength degradation would not significantly affect drift response (BSC 2004, Section 6.4.2.2.2.2).

The drift stability for seismic loading combined with thermal loading and time-dependent strength degradation is analyzed for 80 years (i.e., the time when the thermally induced stresses reach the maximum) and 10,000 years as the occurrence times of the seismic events. In the first step of the analysis, the evolution of damage and rockfall for thermally induced stresses and time-dependent strength degradation are simulated quasi-statically until the time of occurrence of the seismic event is reached. The second step of the analysis accounts for the dynamic effects of the seismic event. The initial state for the dynamic analysis is the equilibrium state that includes the stress state and the damage and rockfall from the model evolution up to the time of the seismic event. Thus, potentially weakened (damaged) lithophysal rock mass around the emplacement drifts due to the previous stress history is subjected to stress changes and inertial forces resulting from seismic ground motions. Seismic shaking can cause additional rockfall and/or damage of the rock mass depending upon: (1) the intensity of the seismic shaking, (2) the category of the lithophysal rock mass (i.e., strength and stiffness), and (3) the level of accumulated damage (a result of previous quasi-static stress and strength-degradation history).

1.2 EFFECTS OF 10^{-4} SEISMIC SHAKING ON DAMAGE IN LITHOPHYSAL ROCK MASS FOR *IN SITU* CONDITIONS

Previous analysis has shown (BSC 2004, Section 6.4.2.2.1 and Figure 1) that seismic ground shaking with 10^{-4} probability of annual exceedance for *in situ* conditions (i.e., ambient temperature and no time-dependent strength degradation) causes damage and rockfall in lithophysal rock mass Category 1 only. The main effect of seismic shaking in lithophysal rock mass Category 1 is to shake down already fractured and potentially loose rocks from the drift walls. The *in situ* stress concentrations in the drift walls exceed the strength of Category 1 lithophysal rock mass, resulting in damage and fracturing in the drift walls to a depth of 0.5 m (BSC 2004, Figure 7-26).

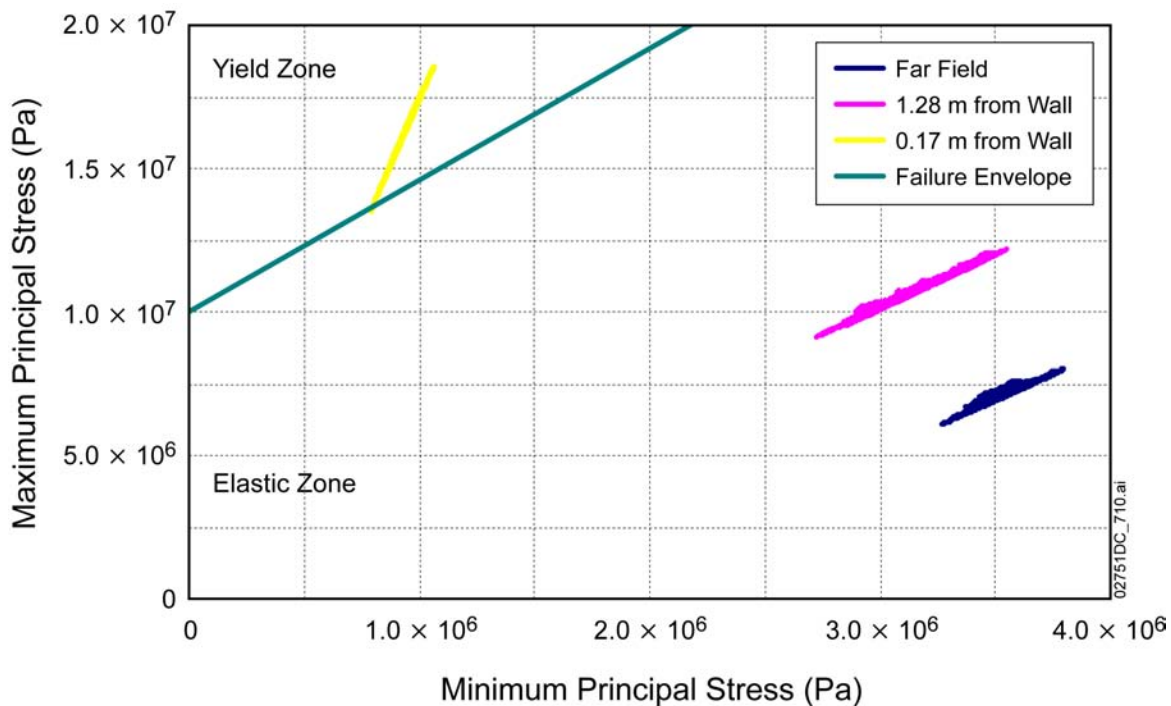
As shown in Figure 1, the 10^{-4} seismic events will shake down some of the loose rock from the walls. The same figure also indicates extension of the damage with development of the breakout. (The breakout is the change of the drift profile due to rockfall of the fractured rock. The extended damage caused by the breakout are the cracks around the breakout in the left wall, shown as red lines.) However, the elastic stress paths in the drift wall during a 10^{-4} seismic event compared to the yield surface for lithophysal rock mass Category 1, shown in Figure 2, indicate that the additional fracturing during shaking is not a consequence of seismically induced stress fluctuations or inertial forces. That is, stress oscillations are relatively small, and do not exceed the yield surface at the points that are outside the yield surface under *in situ* conditions. The additional fracturing is a result of stress redistribution due to removal by shaking of the loose rock. The fractured and potentially loose rock under *in situ* conditions stays in place under quasi-static conditions prior to the first seismic event, providing some confinement and preventing further propagation of damage in the drift walls. When that loose rock is shaken down, the confinement is lost, resulting in additional damage in the form of loss of interblock cohesion (in red), as shown in Figure 1.



Source: BSC 2004, Figure 6-120.

NOTE: Red lines indicate block bonds (cohesion between blocks) that have failed in shear or tension.

Figure 1. Drift Outline and Damage after Simulation of 10^{-4} Ground Motion in Rock Mass Category 1



Source: BSC 2004, Figure 6-121.

Figure 2. Elastic Stress Paths in the Drift Wall Due to 10^{-4} Preclosure Ground Motion: Category 1

In lithophysal rock mass Categories 2 through 5, the analyses indicate that 10^{-4} seismic ground motion under *in situ* conditions causes no damage or rockfall (BSC 2004, Section 6.4.2.2.1). That observation is further confirmed by a series of analyses of drift stability at the 0.4 m/s peak ground velocity (PGV)² level (SNL 2007, Appendix C, Figure C-1). Those analyses show that only four realizations (different combinations of ground motion set and lithophysal rock mass category), all of which are for Category 1, result in some rockfall prediction. (The combinations of ground motion numbers and rock mass categories for different realizations from SNL 2007, Appendix C, Figure C-1, are listed in BSC 2004, Table 6-44.) No rockfall or damage is predicted in lithophysal rock mass Categories 2 to 5. Because lithophysal rock mass Category 1 is relatively sparse (BSC 2004, Section E4.1.3.2 and Figure E-10) and typically occurs within relatively small volumes (i.e., the drift stability model in which the entire drift is in lithophysal rock mass Category 1 significantly overestimates the continuous spatial extent of Category 1), it is expected that seismic ground motion at the 0.4 m/s PGV level or 10^{-4} probability of annual exceedance will not cause additional damage or fracturing in the lithophysal rock around the

² Stability of the emplacement drifts in lithophysal units during preclosure seismic ground motions has been analyzed and documented in Section 6.4.2.2.1 of *Drift Degradation Analysis* (BSC 2004). The analyses were carried out for two preclosure levels of annual probability of exceedance, 5×10^{-4} (the 0.19 m/s PGV level) and 10^{-4} (the 0.384 m/s PGV level). One three-component set of ground motion time histories was provided for each PGV level. In order to capture the effect of spectral content and the duration of time histories on rockfall prediction, the additional analyses were conducted (SNL 2007, Appendix C) for 15 ground motion sets at the 0.4 m/s PGV level, generated by rescaling the ground motions from the 1.05 m/s PGV level by the factor $0.4 / 1.05 \approx 0.381$.

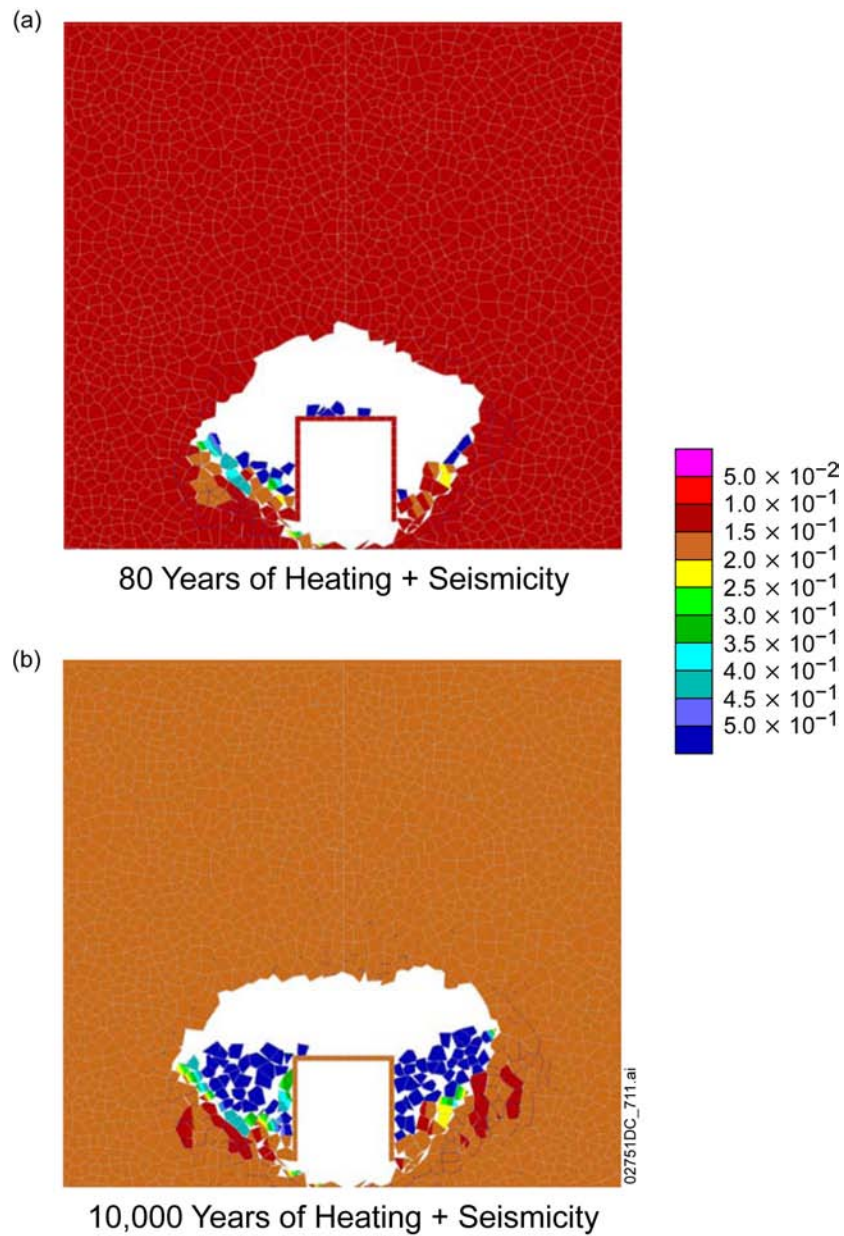
emplacement drifts. However, such ground motions shake down loose blocks created by fracturing due to thermally induced stresses (or time-dependent strength degradation) as shown by additional rockfall from the drift crown in Category 5 lithophysal rock mass after 80 years of heating (BSC 2004, Figure 6-145).

1.3 CUMULATIVE EFFECTS OF MULTIPLE LOADING CONDITIONS

The cumulative effect of combined thermal stresses, time-dependent strength degradation, and single and multiple 10^{-4} ground motions is analyzed for lithophysal rock mass Categories 2 and 5, representative of expected conditions in the repository (BSC 2004, Section S3.4.3). Lithophysal rock mass Category 1 was not analyzed because it represents a relatively small fraction (3%) of lithophysal rock mass (BSC 2004, Section 6.7.1.2) and does not occur in volumes large enough to encompass an entire emplacement drift. Thus, observations of fracturing in rock mass Category 1 in Figure 1 are not relevant for the results for Category 2 shown in Figures 3 and 4. In addition, the impact of a single seismic event on rock mass Category 5 caused only minor rockfall and no additional damage (BSC 2004, Figures S-46 and S-48). Thus, multiple seismic events for rock mass Category 5 were not analyzed.

Multiple seismic events were considered occurring shortly after 80 years and 10,000 years. The states at those two times bound the stresses (relatively large at 80 years compared to 10,000 years) and damage due to time-dependent strength degradation (gradually increasing with time) of the rock mass around the emplacement drifts during the entire 10,000 year period. Thus, the effect of multiple seismic events at intermediate times will be bounded by the effects of the multiple seismic events after 80 years and 10,000 years. When the results are compared for a single and two successive seismic events after 80 and 10,000 years, as shown in Figures 3 and 4, it is obvious that the second seismic event after 80 years causes additional rockfall, while after 10,000 years it does not. However, even when the second event results in additional rockfall, it is relatively small. Because the first two 10^{-4} seismic events shake down loose, fractured rock mass, but do not cause new damage of the rock mass, the subsequent events of the same severity will not cause additional rockfall (and, therefore, were not analyzed).

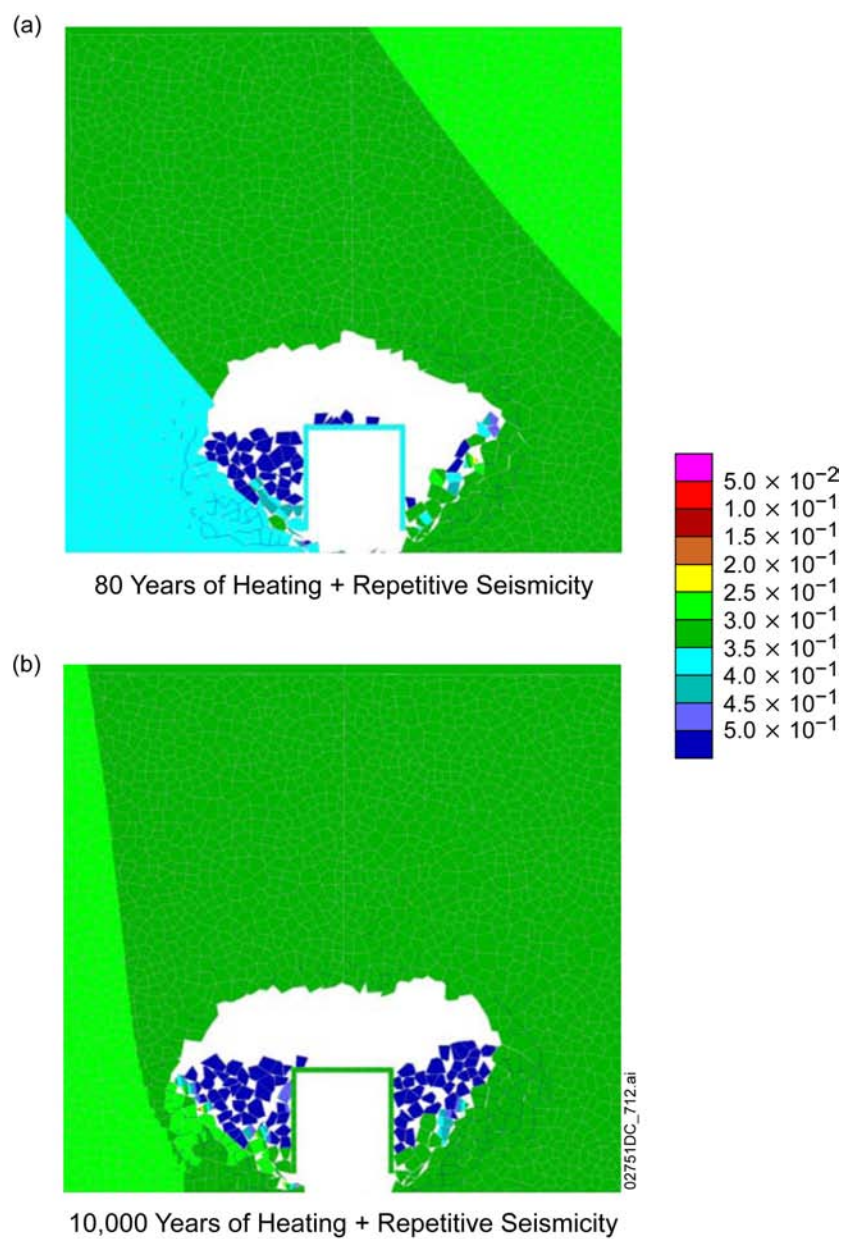
After 80 years, the damage and stress state in the rock mass are such that a single event is insufficient to shake down all of the fractured or loose rock mass. At this time, stresses in the crown are greater than after 10,000 years, providing more confinement and frictional resistance. Consequently, there is additional rockfall after the second seismic event. However, after 10,000 years, the first event shakes down all fractured rock and subsequent events do not cause any additional damage or rockfall.



Source: BSC 2004, Figures S-45 and S-47.

NOTE: A residual, rigid body translation of the model occurred because the dynamic simulation was stopped before the end of the ground motion was reached.

Figure 3. Effect of 10^{-4} Ground Motions in Category 2: Contours of Displacement (m)



Source: BSC 2004, Figure S-49.

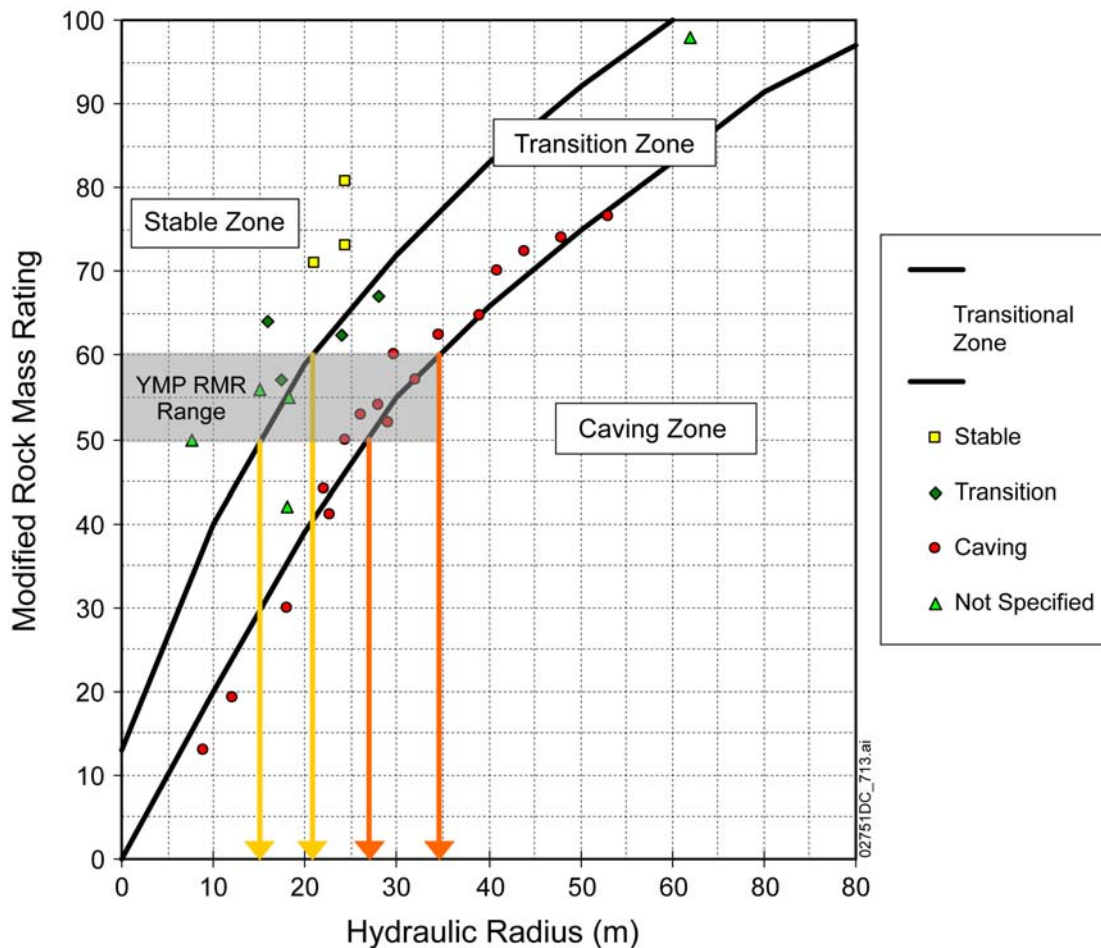
NOTE: A residual, rigid body translation of the model occurred because the dynamic simulation was stopped before the end of the ground motion was reached.

Figure 4. Effect of Two Successive 10^{-4} Ground Motions in Category 2: Contours of Displacement (m)

1.4 COMPARISON WITH CAVING DATA

Empirical mining-industry data describing the potential for caving under *in situ* stress conditions related to rock mass quality, expressed in terms of Geological Strength Index (GSI) or Rock Mass Rating (RMR), and size of excavation, expressed in terms of hydraulic radius (equal to tunnel radius in the case of cylindrical excavations), are shown in Figure 5. Two lines defining three regions are fit through the data. The regions represent: (1) stable excavations; (2) transitional excavations in which some instability may occur, but not caving or collapse of the excavation; and (3) excavations that cave. As expected, the data indicate that with a reduction of rock mass quality, smaller spans (or radii) of excavations are required to ensure stable excavations. The range of RMR for the lithophysal rock mass at Yucca Mountain, which is estimated to be approximately 50 to 60 (BSC 2004, Section 6.4.2.4.1.2), is indicated in Figure 5. The radius of a cylindrical tunnel that would cave in lithophysal rock mass is between approximately 25 and 35 m. A transitional zone between stable excavations and caving for the lithophysal rock RMR range is for hydraulic radii greater than 15 to 20 m.

The emplacement drift radius in the initial configuration is 2.75 m. After 10,000 years of heating, time-dependent strength degradation and 10^{-4} seismic ground motions, the maximum span increases to approximately 8.5 m (Figure 4). The corresponding hydraulic radius of 4.25 m, although greater than the initial radius of 2.75 m, is still approximately 3.5 times smaller than the minimum hydraulic radius (15 m) for the transitional region when some instability under *in situ* conditions is expected to occur. The drift degradation and associated increase in the hydraulic radius from 2.75 to 4.25 m result in an increase in the caving potential, but this increase is insufficient to result in instability or caving under *in situ* stress conditions. The results of the numerical simulations are consistent with the empirical data. The model does not predict instability of the excavation under *in situ* stress conditions either in the initial configuration or after an increase in the tunnel span to 8.5 m.



Source: BSC 2004, Figure 6-149.

NOTE: Caving potential is expressed in terms of the modified rock mass rating and hydraulic radius. Modified rock mass rating is equivalent to rock mass rating in the case of Yucca Mountain excavations. Stable and caving regions are separated by a transition zone. The yellow lines represent the lower and upper bounds (for the range or RMR between 50 and 60, respectively) of the hydraulic radius corresponding to the transition zone; the orange lines represent the lower and upper bounds (for the range or RMR between 50 and 60, respectively) of the hydraulic radius corresponding to the caving zone.

Figure 5. Excavation Dimensions Required for Caving Gained from Mining Experience

1.5 CONCLUSION

Seismic ground motions with 10^{-4} probability of annual exceedance (or the 0.4 m/s PGV level) cause rockfall in lithophysal rock mass Category 1 under *in situ* conditions. This rockfall is mostly a result of the shaking down of already fractured rock mass in the drift walls under *in situ* stress conditions. Any additional damage or fracturing of Category 1 rock is not directly a result of seismically induced transient stress changes or inertial forces, but a consequence of unraveling of previously fractured rock and loss of confinement. These ground motions do not cause new damage or rockfall in lithophysal rock mass Categories 2 to 5 under *in situ* conditions.

Depending on the stress state and level of damage (fracturing) of the rock mass at the time of seismic events, multiple events may or may not cause additional rockfall. The analyses show that in lithophysal rock mass Category 2, a second event after an initial event at 80 years causes additional rockfall, while after an initial event at 10,000 years additional rockfall after the second event does not occur. The analysis of multiple events in Category 5 has not been carried out because single events after 80 years and 10,000 years cause minor rockfall.

Results from numerical analysis of emplacement drifts are consistent with empirical data of underground excavation stability under *in situ* stresses as a function of hydraulic radius and rock mass quality rating. The increased hydraulic radius (4.25 m) after a seismic event at 10,000 years is still much smaller than the limit (15 m) when instability under *in situ* conditions is expected.

2. COMMITMENTS TO NRC

None.

3. DESCRIPTION OF PROPOSED LA CHANGE

None.

4. REFERENCES

BSC (Bechtel SAIC Company) 2004. *Drift Degradation Analysis*. ANL-EBS-MD-000027 REV 03. Las Vegas, Nevada: Bechtel SAIC Company. ACC: DOC.20040915.0010; DOC.20050419.0001; DOC.20051130.0002; DOC.20060731.0005; LLR.20080311.0066.

SNL (Sandia National Laboratories) 2007. *Mechanical Assessment of Degraded Waste Packages and Drip Shields Subject to Vibratory Ground Motion*. MDL-WIS-AC-000001 REV 00. Las Vegas, Nevada: Sandia National Laboratories. ACC: DOC.20070917.0006; DOC.20080623.0002; DOC.20081021.0001.

RAI Volume 3, Chapter 2.2.1.3.2, Fourth Set, Number 2:

Demonstrate that the dimensions of the tessellated domain in the UDEC-Voronoi model do not affect significantly the calculations of rockfall volume from seismic events.

Basis: The upper boundary of the tessellated domain in UDEC-Voronoi model is set 10.25 m above the initial drift roof (BSC, 2004, Figure 6-116). However, contours of block displacement magnitude intersect the upper boundary of the tessellated domain, indicating that some additional displacement occurs outside this domain (e.g., BSC, 2004, Figure 6-176). Also, plots of the final position of the Voronoi blocks after an analysis (e.g., BSC, 2004; Figures P-17, P-18, and P-24) indicate blocks at the top of the model could be predicted to separate from the overlying elastic domain, which would suggest the caved zone might have extended higher if the model upper boundary had been higher. DOE does not provide a technical basis for the selecting the dimensions of the tessellated domain, and does not provide sensitivity analyses in BSC (2004, section 6.4.2.1) to demonstrate that uncertainty in the dimensions of the tessellated domain do not affect significantly the calculations of rockfall volume during seismic events.

1. RESPONSE

Analyses of emplacement drift stability in the lithophysal rock mass during strong seismic ground motions were carried out in a UDEC Voronoi model in which the region of the rock mass around the drift was represented as an assembly of Voronoi blocks (i.e., the domain was tessellated into Voronoi blocks). This region extends 4.25 m from the drift walls laterally and 10.25 m above the drift crown (BSC 2004, Figure 6-116). The remainder of the model, outside the tessellated domain, was considered to deform elastically. Thus, the model assumption was that inelastic deformation of the lithophysal rock mass, in particular, large deformation associated with fracturing, damage, and unraveling of rock mass, is contained within the tessellated domain.

The size of the tessellated domain and distance of its boundaries from the drift walls was determined from the preliminary simulations and an estimate of the maximum size of the caved region (or the rockfall volume), which must be completely contained within the tessellated domain. Because the model does not allow the caved region to propagate beyond the boundaries of the tessellated region, the assumed size of the tessellated region was confirmed to be sufficiently large that the caved region does not propagate to the boundaries of the tessellated region.

The perimeter of the caved region is contained within the tessellated region and large displacements and disintegration of the rock mass associated with collapse of the emplacement drift do not propagate to the boundaries of the tessellated region (e.g., BSC 2004, Figures 6-176 and P-25). In examples of quasi-static drift degradation sensitivity analysis in which the maximum collapse is induced by degrading rock mass strength to zero, an increase in size of the

tessellated domain does not affect the rockfall volume or the caved region size. That is, the caved region remains contained within the original tessellated region.

1.1 ROCKFALL VOLUME COMPARED TO SIZE OF TESSELLATED REGION

The configuration of the emplacement drift and displacement contours after drift collapse and shaking by a seismic event¹ with a 10^{-4} probability of annual exceedance is shown in Figure 1. The figure also shows the outline of the region tessellated in the Voronoi blocks. The contours of certain displacement values (e.g., greater than 0.1 m, as shown as the brown region in Figure 1) cross the upper boundary of the tessellated domain, indicating that additional displacement occurs outside this domain. The reasons for deformation outside the tessellated region are the following:

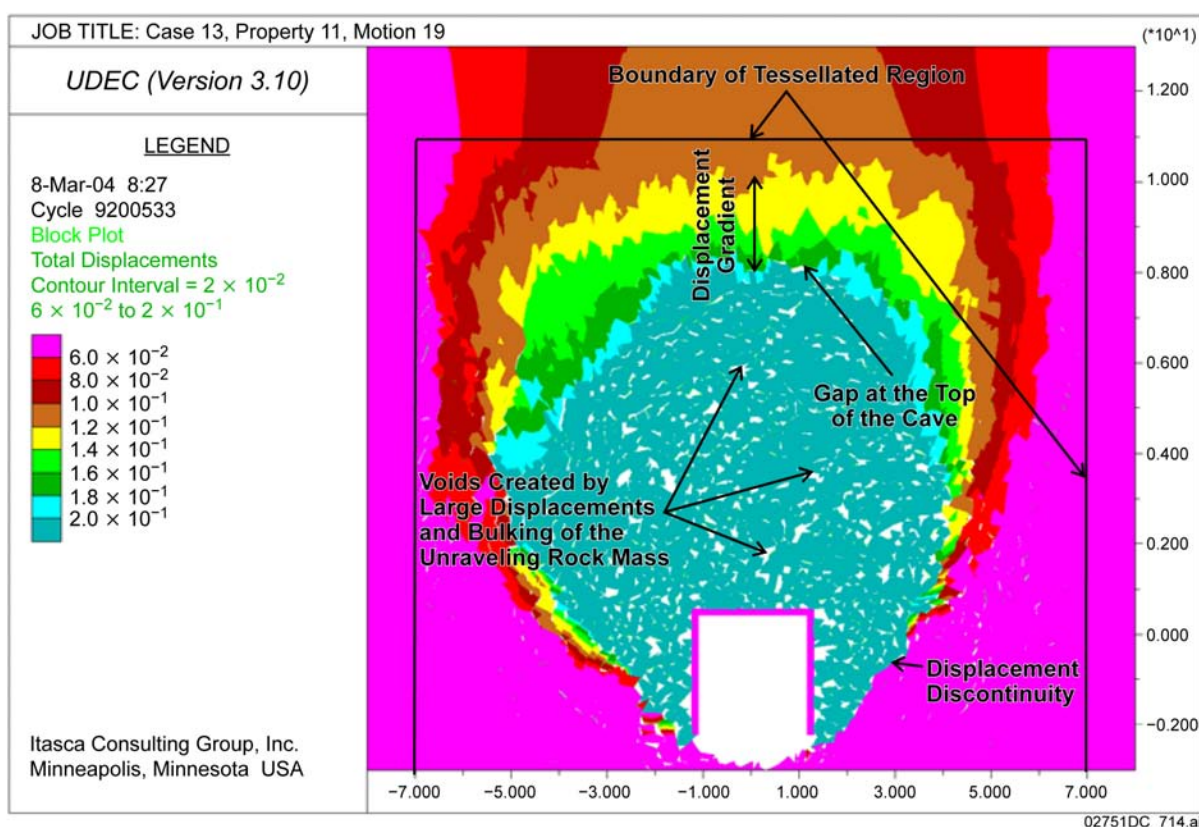
1. The material outside the tessellated domain is elastic, lithophysal rock (Category 1) with a relatively small Young's modulus of 1.9 GPa (BSC 2004, Table E-11), and it deforms in response to deformation and change in stresses as the drift degrades.
2. The boundary condition on the top of the model, as shown in Figure 6-117 of *Drift Degradation Analysis* (BSC 2004), is the stress boundary condition (equal to the overburden weight). In addition, as can be seen from the same figure and in Figure 6-139 of the analysis (BSC 2004), the height of the model above the drift is relatively small (i.e., 17.5 m above the drift axis). As a consequence, the model generally overestimates deformation and, in particular, bending deformation of the elastic part of the model above the caved region as the emplacement drift degrades. (In the model of a finite size representing infinite half-space, the model boundaries are located at a distance from the excavation where displacements are expected to be small. However, if the stress boundary condition is used on those boundaries, the displacements inside the model will be overestimated because the strength and stiffness of the rock outside the model domain are neglected.)

However, deformation of the elastic overburden (as indicated in Figure 1) does not mean that the caved region expanded to the boundary of the tessellated region, or that the boundary affected the size of the caved region. If a boundary effect were present, gaps would occur along the boundary of the tessellated region. These gaps would be manifested in the displacement contours as displacement discontinuities or regions of large displacement gradients. As shown in Figure 1, the displacement discontinuities and regions of large displacement gradients are

¹ The term "seismic event" in this response generally refers to the ground motion caused by an earthquake. In the context of postclosure seismic consequence analyses, the ground motion is typically characterized by the peak ground velocity (PGV) value of its first horizontal component. For a given value of horizontal PGV, the probabilistic seismic hazard analysis for Yucca Mountain, combined with ground motion conditioning and site-response modeling, gives a mean annual frequency with which the peak velocity value is expected to be exceeded (the bounded hazard curve). Seismic event rates refer, therefore, to ground motion exceedance rates rather than earthquake occurrence rates. For convenience, sets of three-component ground motion time histories are sometimes referred to in terms of their horizontal PGV value (e.g., 0.4 m/s PGV ground motions) or the mean annual frequency of the horizontal PGV value being exceeded (e.g., 10^{-4} ground motions).

completely contained within the tessellated region. Moreover, the displacement field crossing the boundary of the tessellated region is continuous, indicating that near the boundary the tessellated region and the outside elastic domain are mechanically equivalent and deform continuously.

Voids resulting from large block displacements exist in the contour plots and appear as white spaces between the blocks. The voids are consequences of unraveling of rock mass and large displacements that include block rotations. Figure 1 indicates that most of the voids are contained within the region where displacements are 0.2 m or greater and that all of the voids are completely contained within the boundary of the tessellated region. No major voids have been identified in the vicinity of the boundary of the tessellated region.

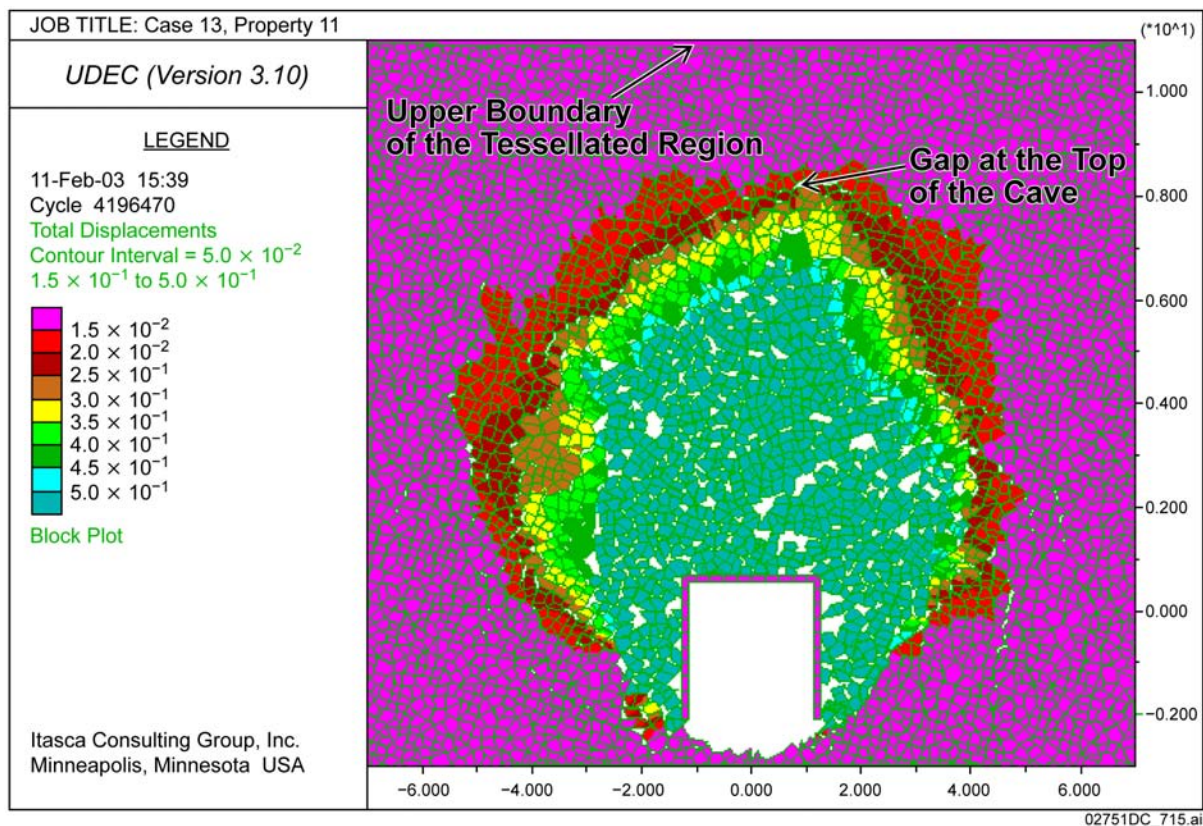


Source: BSC 2004, Figure 6-176.

NOTE: The y-coordinate of the top of the tessellated domain is 11 m; horizontally, the tessellated domain extends between -7 m and 7 m. Displacement contours in this figure quantify the displacement between a particle's initial and final position during the simulation.

Figure 1. Contours of Displacement (m) for Previously Collapsed Drift after Subsequent Shaking by Ground Motions with 1×10^{-4} Probability of Annual Recurrence

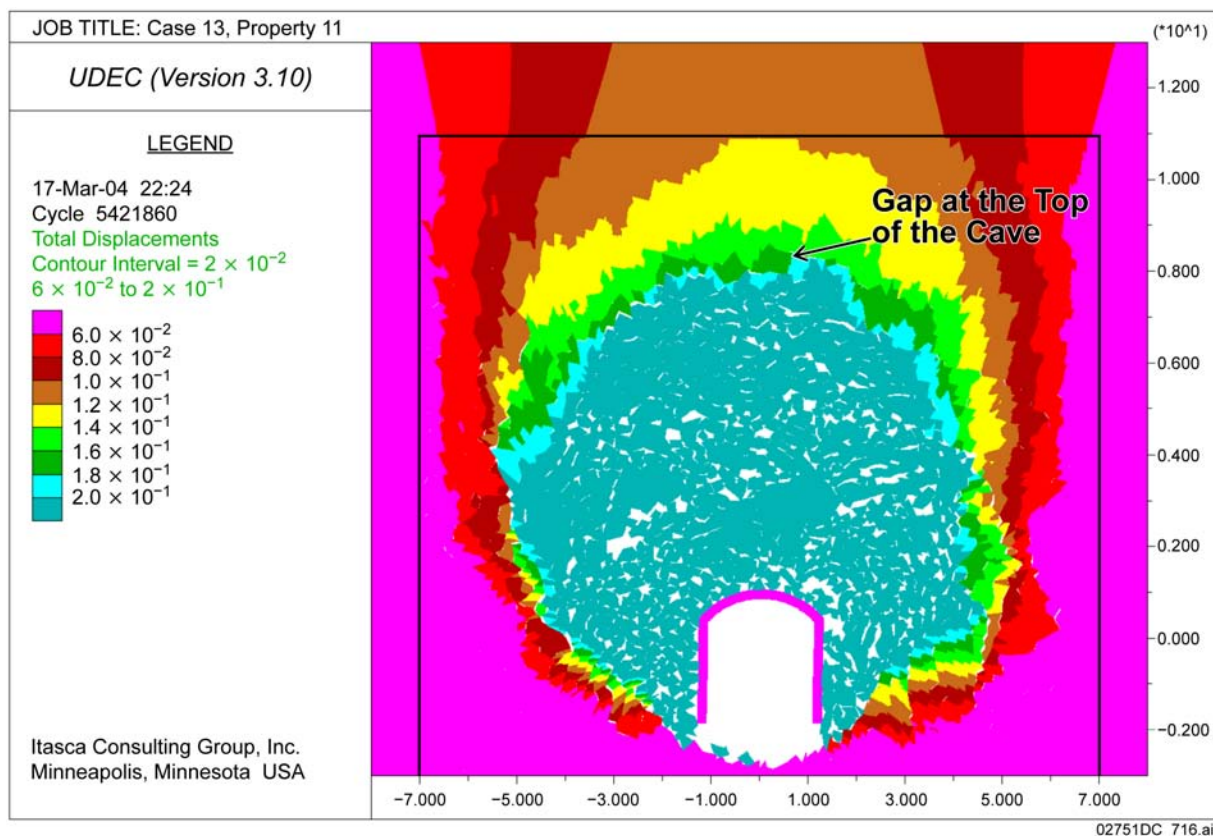
The drift configuration and displacement contours for the case of quasi-static drift degradation for 0.2-m Voronoi block size (response to RAI 3.2.2.1.2.1-6-002) with a rigid, rectangular representation of the drip shield (BSC 2004, Section P2.2.2) are shown in Figure 2. In these calculations, carried out for lithophysal rock mass Category 1, the quasi-static drift collapse is simulated by gradual reduction to zero of the cohesion and tensile strength of the contacts between the blocks. The stress tensor field for the same case is shown in Figure P-17 of *Drift Degradation Analysis* (BSC 2004). The spatial extent of Figure 2 roughly coincides with the tessellated domain. Because the lower bound of displacement contours is set to 0.15 m, the contours of smaller displacements are not differentiated. However, Figure 2 indicates that large displacements of blocks are entirely contained within the tessellated region and that in the vicinity of the boundary of the tessellated domain, the blocks do not undergo the large displacements that would result in formations of voids between the blocks.



NOTE: The y-coordinate of the top of the tessellated domain is 11 m; horizontally, the tessellated domain extends between -7 m and 7 m. Displacement contours in this figure quantify the displacement between a particle's initial and final position during the simulation.

Figure 2. Displacement Contours (m) for Quasi-Static Drift Degradation, 0.2-m Average Block Size

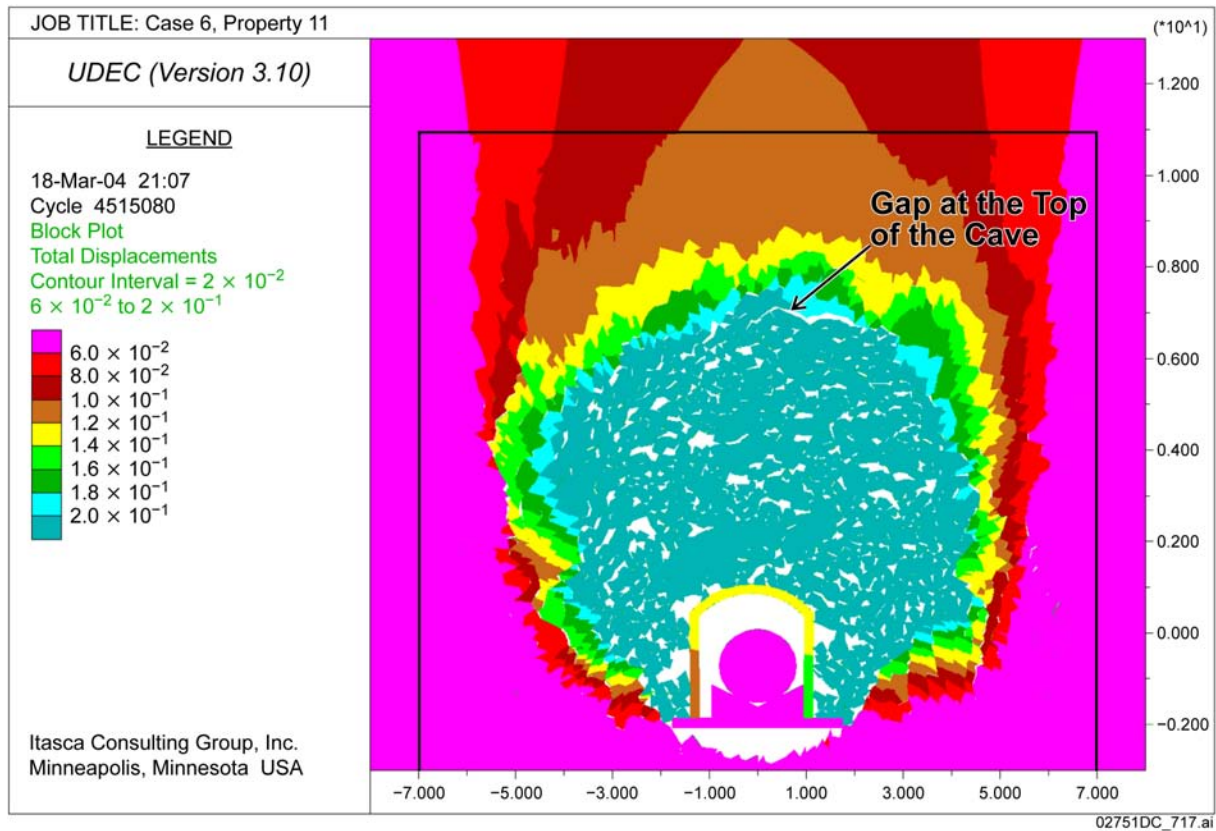
The displacement contour plots for two models with configurations and stress tensor plots shown in Figures P-18 and P-24 of *Drift Degradation Analysis* (BSC 2004) are shown in Figures 3 and 4, respectively. The figures also include the outline of the tessellated domain. The displacement fields are continuous across the boundary of the tessellated domain, and block separation from the boundary is not indicated. The voids created by unraveling of the rock mass are completely contained within the tessellated domain. The indicated gap at the top of the caved region is well away from the upper boundary of the tessellated domain.



Source BSC 2004, Figure P-19.

NOTE: The black lines indicate the boundary of the tessellated region. The y-coordinate of the top of the tessellated domain is 11 m; horizontally, the tessellated domain extends between -7 m and 7 m. Displacement contours in this figure quantify the displacement between a particle's initial and final position during the simulation.

Figure 3. Quasi-Static Drift Degradation, 0.2-m Average Block Size: Contours of Displacement (m) for Deformable Drip Shield with Arched Top, Pinned Bottom, No Invert



Source: BSC 2004, Figure P-25.

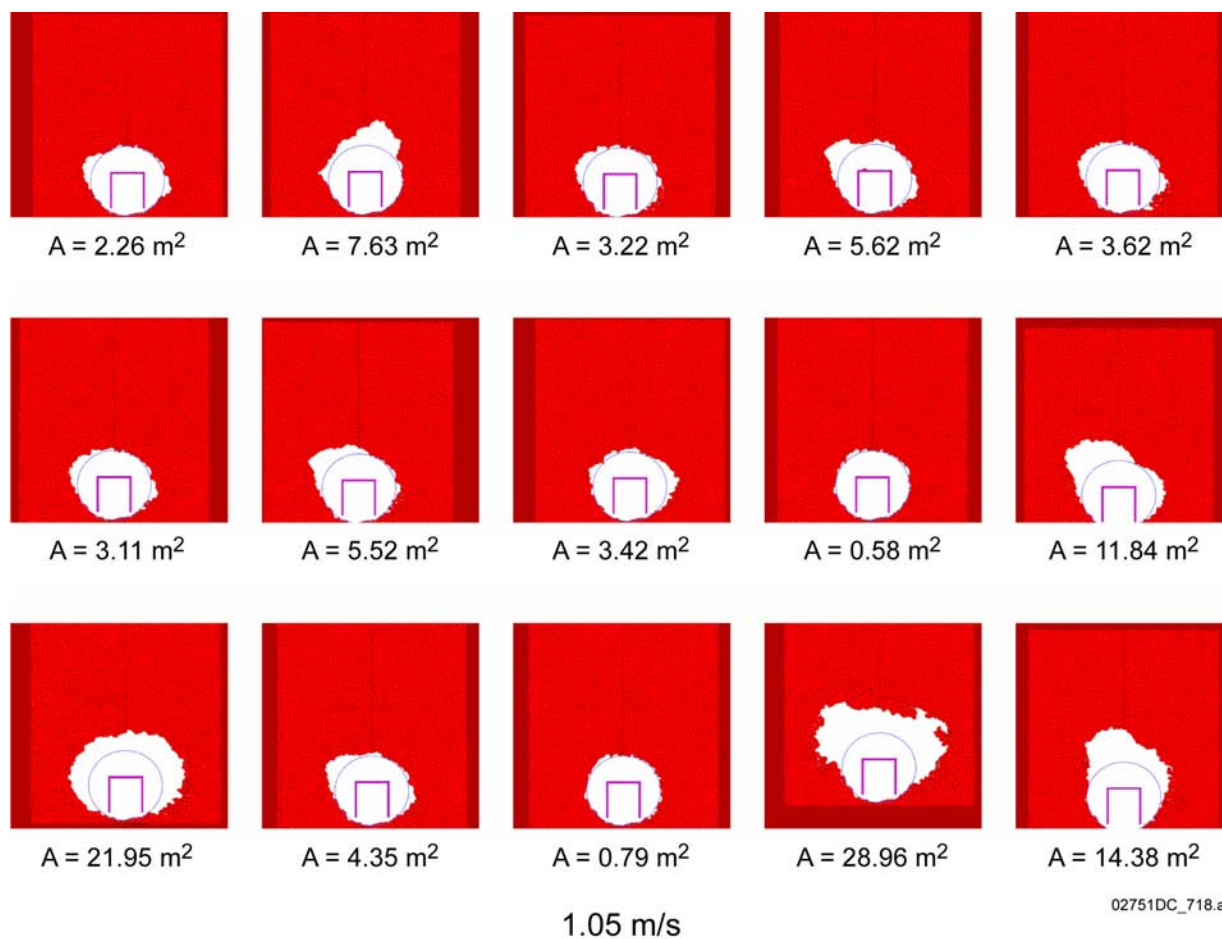
NOTE: The black lines indicate the boundary of the tessellated region. The y-coordinate of the top of the tessellated domain is 11 m; horizontally, the tessellated domain extends between -7 m and 7 m. Displacement contours in this figure quantify the displacement between a particle's initial and final position during the simulation.

Figure 4. Quasi-Static Drift Degradation, 0.2-m Average Block Size: Contours of Displacement (m) for Deformable Drip Shield with Arched Top, Bottom Rests on the Invert

1.2 SIZE OF THE CAVED REGION AFTER SEISMIC EVENTS

Seismically induced rockfall and stable drift profiles in the lithophysal units are calculated for the 0.4, 1.05, and 2.44 m/s peak ground velocity (PGV) levels. The details of the calculations and the results are presented in *Mechanical Assessment of Degraded Waste Packages and Drip Shields Subject to Vibratory Ground Motion* (SNL 2007a, Appendix C). At each PGV level, 15 simulations are carried out for different combinations (provided in BSC 2004, Table 6-44) of the ground motion sets and the lithophysal rock mass categories.

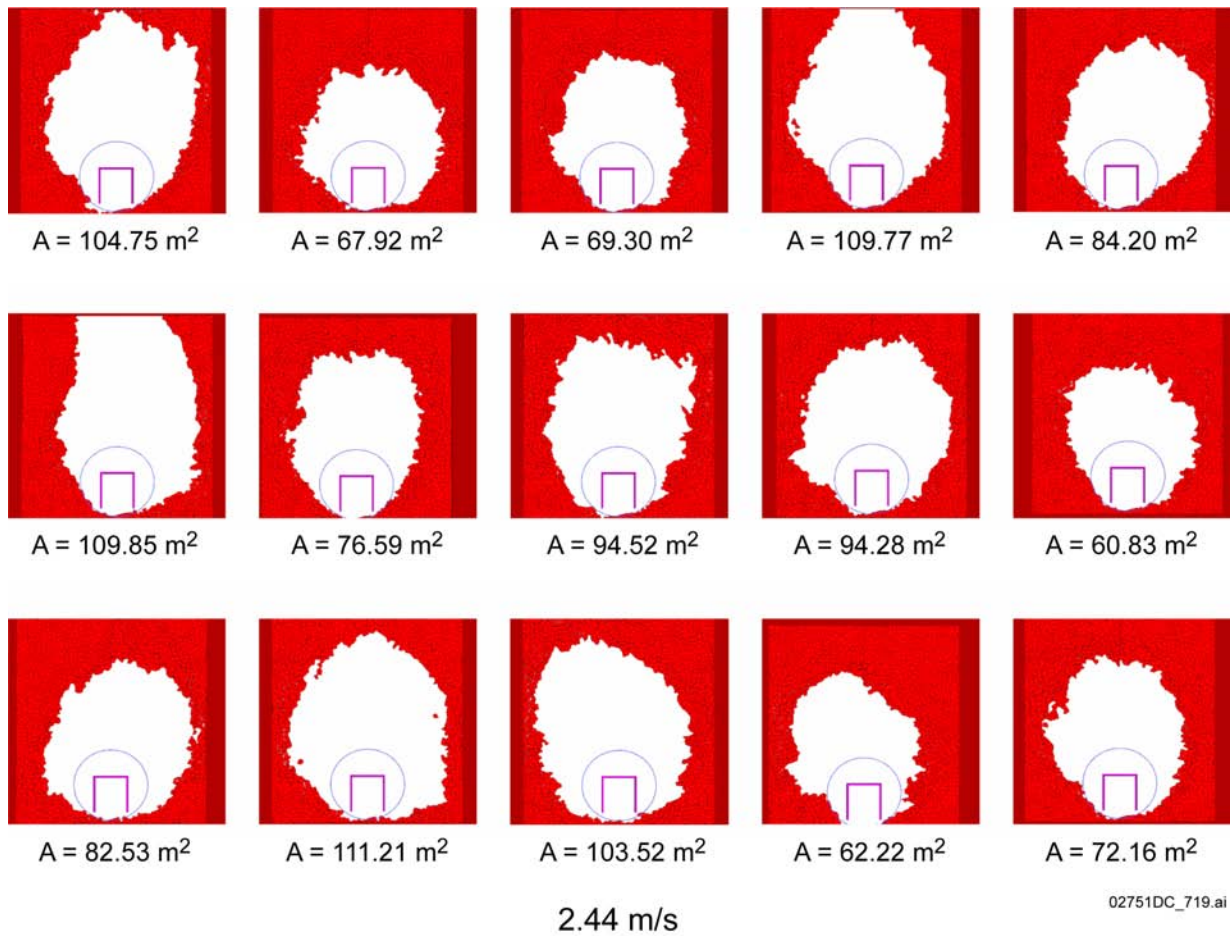
The stable drift profiles for the 1.05 and 2.44 m/s PGV levels are shown in Figures 5 and 6, respectively. The ground motions on the 0.4 m/s PGV level are not shown here, but these rarely cause rock-fall (SNL 2007a, Figure C-1). When rock-fall occurs at the 0.4 m/s PGV level, the amounts are small and only occur in Category 1 lithophysal rock mass, which is such a small fraction of the repository host rock (SNL 2007b, Section 6.7.1.2). The plots show, in red, the part of the model domain with displacement less than 0.1 m relative to the reference point, which is moving as the far field, defined by the incoming seismic ground motions. The threshold of 0.1 m was used irrespective of the rock mass category. However, the results in Section 1.1 show that a 0.1-m threshold results in an overestimate of the caved region in Category 1 rock (e.g., Figure 1). Category 1 rock is the weakest rock category and represents only a small portion of the total rock mass (BSC 2004, *Executive Summary*). It is not expected to comprise the entire perimeter for any single section of emplacement drift. The low stiffness of this category (less than a third of the stiffness of the next stronger rock mass, Category 2 rock) (BSC 2004, Table E-11) results in large displacements (greater than 0.1 m) after drift collapse even in the elastic domain. Consequently, realizations 4 and 6 of Figure 6, which are for Category 1, predict a caved region extending to the upper boundary of the tessellated domain for the 2.44 m/s PGV level. This PGV value is associated with an annual exceedance frequency of 4.52×10^{-7} (SNL 2007b, Section 6.1.7). The combination of a low annual exceedance frequency and the limited amount of Category 1 rock in the repository drifts (about 3%; SNL 2007b, Section 6.7.1.2) indicates that their effect on rockfall volume estimates is not significant. Combinations of the ground motion sets and rock mass categories for different realizations are provided in Table 6-44 in *Drift Degradation Analysis* (BSC 2004). All other realizations show that the caved region is completely contained within the tessellated domain (delineated in lighter red). These realizations demonstrate that the dimensions of the tessellated domain do not affect, and in particular do not limit, predicted rockfall volumes from seismic events.



Source: SNL 2007a, Figure C-2.

NOTES: Realizations 1 to 5 are in the first row realizations 6 to 10 are in the second row, and realizations 11 to 15 are in the third row, all from left to right. The realization numbers correspond to Table 6-44 in *Drift Degradation Analysis* (BSC 2004). The loose blocks that are part of rockfall are not shown. The rectangular shape inside the drift represents the drip shield. The initial drift outline is shown by blue lines.

Figure 5. Stable Drift Profiles and Rockfall Volumes per Unit Length (shown as cross-sectional areas) for 15 Realizations at the 1.05 m/s PGV Level



Source: SNL 2007a, Figure C-3.

NOTES: Realizations 1 through 5 are in the first row, from left to right; realizations 6 through 10 are in the second row, from left to right; and realizations 11 to 15 are in the third row, from left to right. The realization numbers correspond to Table 6-44 in *Drift Degradation Analysis* (BSC 2004). The loose blocks that are part of rockfall are not shown. The rectangular shape inside the drift represents the drip shield. The initial drift outline is shown by blue lines.

Figure 6. Stable Drift Profiles and Rockfall Volumes per Unit Length (shown as cross-sectional areas) for 15 Realizations at the 2.44 m/s PGV Level

1.3 SENSITIVITY ANALYSES

In the analysis of drift degradation during seismic events, the upper boundary of the tessellated domain is 10.25 m above the initial drift roof. However, in the quasi-static analysis of drift degradation (i.e., the cases discussed in Section 1.1), the upper boundary of the tessellated domain is 8.25 m above the drift roof. A back-analysis of the results of the completed calculations demonstrates that the selected size of the tessellated domain does not affect the results of the calculation and, in particular, does not affect the estimated rockfall volume. To further demonstrate the effect of the dimensions of the tessellated domain on the estimates of rockfall volume, a sensitivity analysis is carried out in which the top of the tessellated domain is 13.25 m above the initial drift roof, and the vertical boundaries of the domain are 7.25 m from

the drift walls. Six quasi-static calculations of drift degradation with increased tessellated domain were carried out for different average block sizes (0.2 and 0.3 m) and block geometry realizations. The geometry used in one of the simulations (0.2-m average block size), indicating the size of the original tessellated domain, is shown in Figure 7.

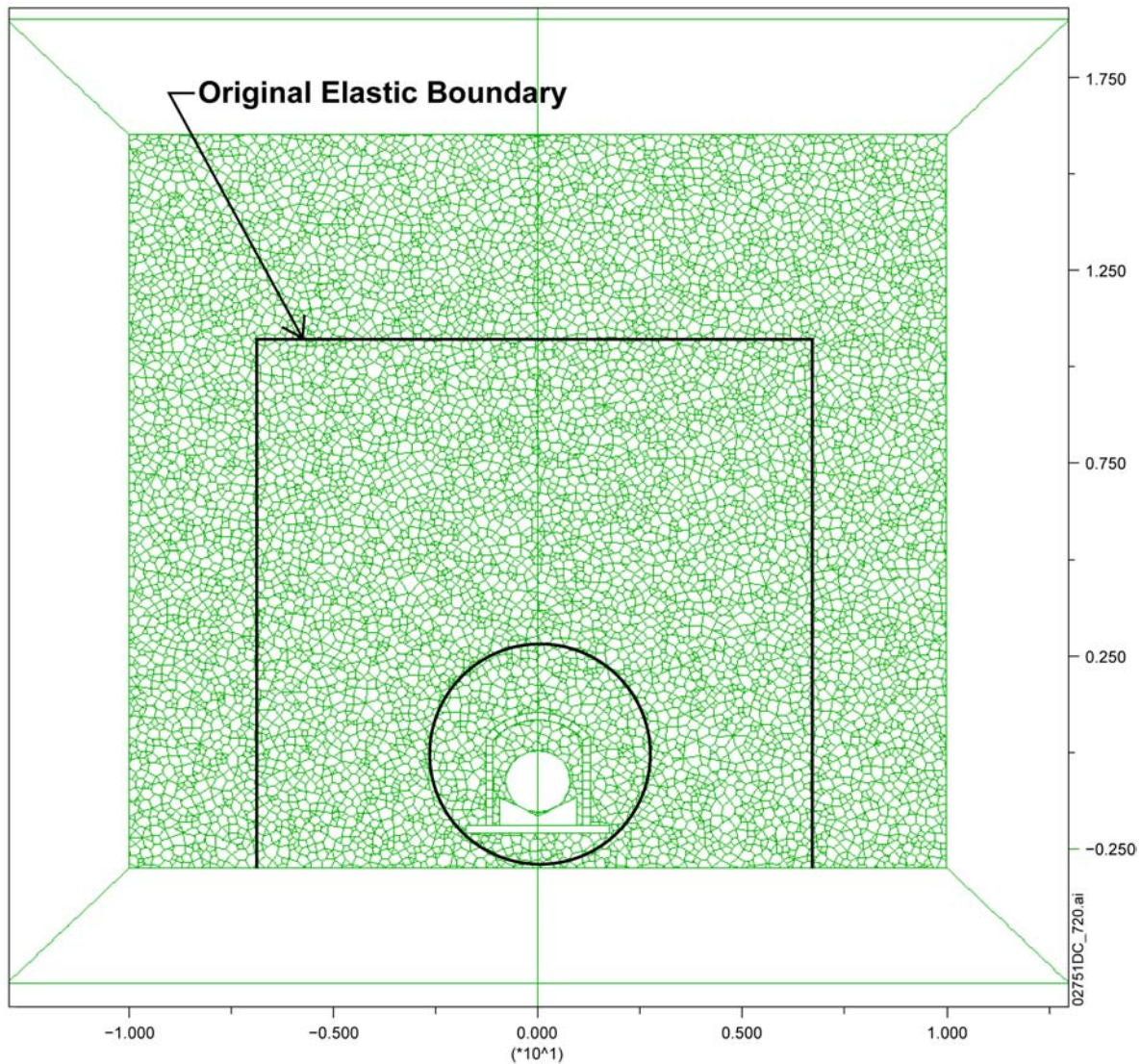
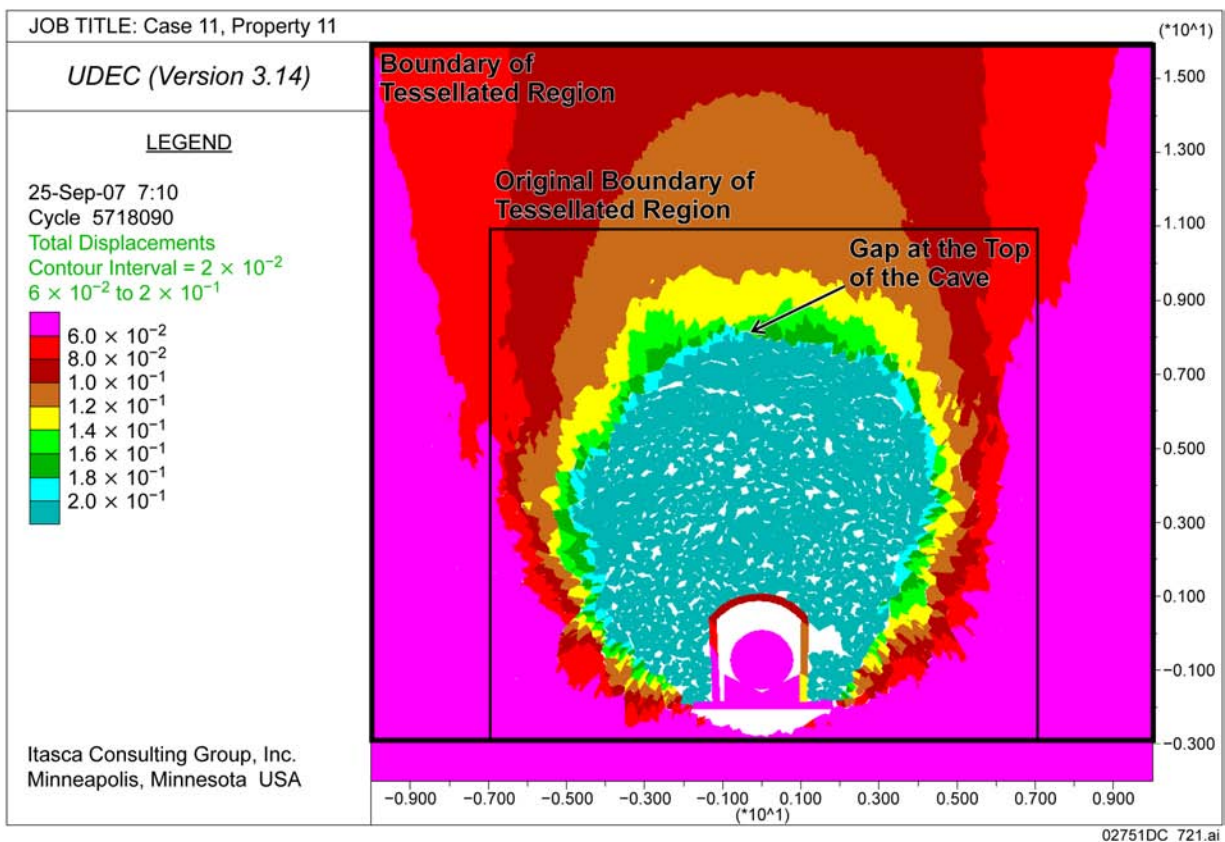


Figure 7. Initial Geometry of the Model with Extension of the Tessellated Domain

The results of one simulation, which are typical for all simulations with increased tessellated domain, are shown in Figures 8 and 9. Figure 8 shows contours of displacement magnitudes. The stress tensors colored by the value of the major principal stress are shown in Figure 9. In both figures, showing the same model domain, the lateral and top boundaries of the view window coincide with the boundaries of the tessellated domain. Also, the outline of the tessellated domain with the boundary 8.25 m above the initial drift roof, as used in the quasi-static analysis of drift degradation, is indicated in both figures.

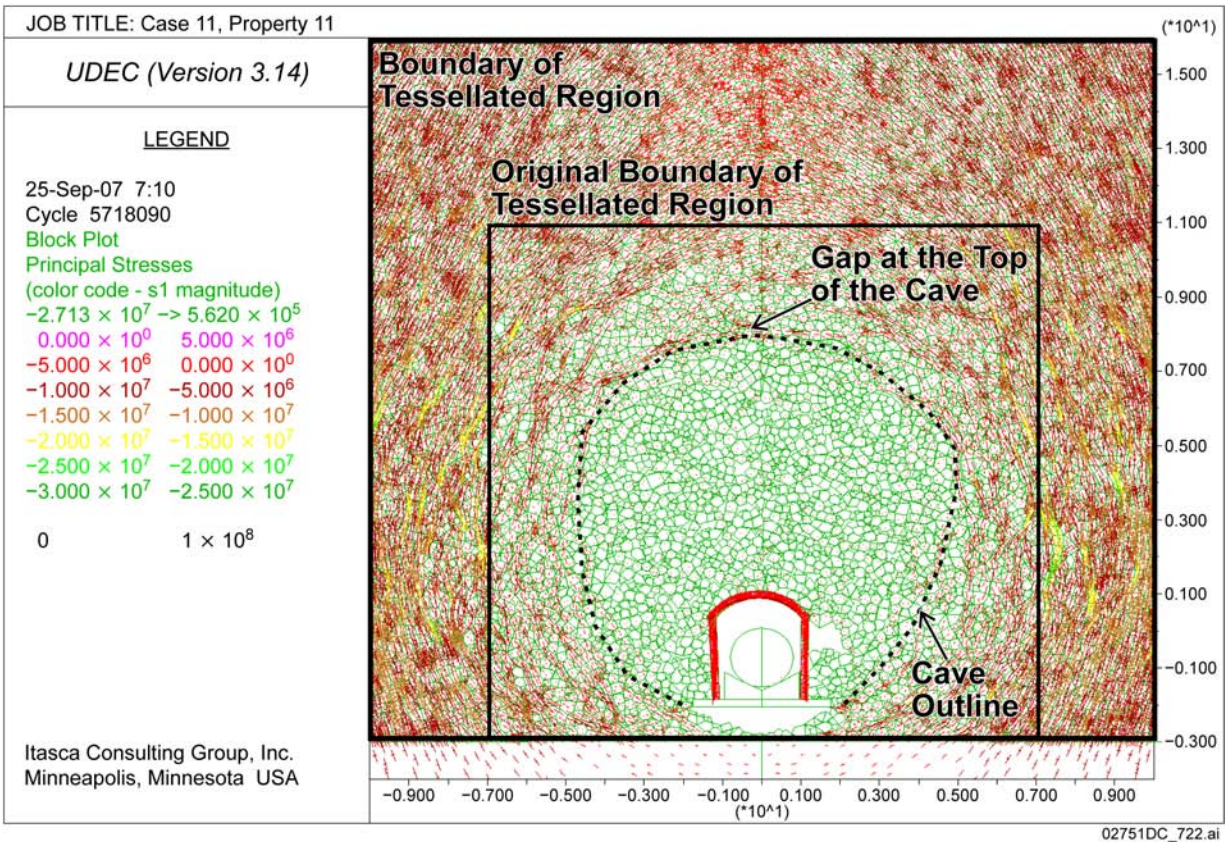
The displacement contour plot shown in Figure 8 is similar to those with a smaller tessellated domain shown in Section 1.1. The location of the top of the caved region is approximately 8 m above the drift center (or 5.25 m above the initial drift roof), irrespective of the size of the tessellated domain (as used in original analyses discussed in Section 1.1 or in these sensitivity analyses).

The stress tensor plot in Figure 9 provides another method for assessment of the size of the rockfall volume and potential effect of the size of the tessellated domain on that volume. The caved region or the rockfall volume is essentially the de-stressed region relative to the stress-bearing region in the stable rock mass. As shown in Figure 9, the distressed region is completely contained within the original (smaller) tessellated domain.



NOTE: The y-coordinate of the top of the tessellated domain is 16 m; horizontally, the tessellated domain extends between -10 m and 10 m. Displacement contours in this figure quantify the displacement between the particle initial and final position during the simulation.

Figure 8. Displacement Contours (m) for Quasi-Static Drift Degradation, 0.2-m Average Block Size, and Extension of the Tessellated Domain



NOTE: The y-coordinate of the top of the tessellated domain is 16 m; horizontally, the tessellated domain extends between -10 and 10 m. The range $-2.713 \times 10^7 > 5.620 \times 10^5$ shown in the legend indicates the range of the major principal stress magnitudes in the plot.

Figure 9. Stress Tensor Field (Pa) Colored by Value of the Major Principal Stress for Quasi-Static Drift Degradation, 0.2-m Average Block Size, and Extension of the Tessellated Domain

1.4 CONCLUSION

The potential effect of the size of the tessellated domain on the estimated rockfall volumes is checked by back-analysis of the model results. As described in Section 1.2 of this response, in all but two of the simulations (Figure 6, realizations 4 and 6), the contour plots of displacement show continuity across the boundaries of the tessellated domain, and the voids and the gaps, which result from bulking of the rock mass as unraveling blocks displace and rotate, are contained within the tessellated domain. The two exceptions are for the weakest rock (Category 1) and PGV values of 2.44 m/s, and for those combinations of rock strength and PGV, the analysis overpredicts the rockfall volume. Sensitivity analyses, conducted with an extended tessellated domain, result in the same estimates of the size of the caved region and rockfall volume as for the original, smaller tessellated domain used in the drift degradation analysis and assessment of the rubble load on the drip shield. Thus, the dimensions of the tessellated domain do not affect the calculations of rock fall volumes from seismic events or during quasi-static drift degradation.

2. COMMITMENTS TO NRC

None.

3. DESCRIPTION OF PROPOSED LA CHANGE

None.

4. REFERENCES

BSC (Bechtel SAIC Company) 2004. *Drift Degradation Analysis*. ANL-EBS-MD-000027 REV 03. Las Vegas, Nevada: Bechtel SAIC Company. ACC: DOC.20040915.0010; DOC.20050419.0001; DOC.20051130.0002; DOC.20060731.0005; LLR.20080311.0066.

SNL (Sandia National Laboratories) 2007a. *Mechanical Assessment of Degraded Waste Packages and Drip Shields Subject to Vibratory Ground Motion*. MDL-WIS-AC-000001 REV 00. Las Vegas, Nevada: Sandia National Laboratories. ACC: DOC.20070917.0006; DOC.20080623.0002; DOC.20081021.0001.

SNL 2007b. *Seismic Consequence Abstraction*. MDL-WIS-PA-000003 REV 03. Las Vegas, Nevada: Sandia National Laboratories. ACC: DOC.20070928.0011, LLR.20080414.0012